Transp Porous Med (2005) 58:23–41
DOI 10.1007/s11242-004-5468-2

Predictive Pore-Scale Modeling of Single and Multiphase Flow

PER H. VALVATNE, MOHAMMAD PIRI, XAVIER LOPEZ and MARTIN J. BLUNT*
Department of Earth Science and Engineering, Imperial College London, SW7 2AZ, U.K.

(Received: 15 August 2003; in final form: 25 February 2004)

Abstract. We show how to predict flow properties for a variety of rocks using pore-scale modeling with geologically realistic networks. The pore space is represented by a topologically disordered lattice of pores connected by throats that have angular cross-sections. We successfully predict single-phase non-Newtonian rheology, and two and three-phase relative permeability for water-wet media. The pore size distribution of the network can be tuned to match capillary pressure data when a network representation of the system of interest is unavailable. The aim of this work is not simply to match experiments, but to use easily acquired data to estimate difficult to measure properties and to predict trends in data for different rock types or displacement sequences.

Key words: multiphase flow, pore-scale modeling, relative permeability

1. Introduction

In network modeling the void space of a rock is represented at the microscopic scale by a lattice of pores connected by throats. By applying rules that govern the transport and arrangement of fluids in pores and throats, macroscopic properties, for instance capillary pressure or relative permeability, can then be estimated across the network, which typically consists of several thousand pores and throats representing a rock sample of a few millimeters cubed.

Until recently most networks were based on a regular lattice. The coordination number can vary depending on the chosen lattice (e.g. 5 for a honeycombed lattice or 6 for a regular cubic lattice). As has been noted by many authors (Chatzis and Dullien, 1997; Wilkinson and Willemsen, 1983) the coordination number will influence the flow behavior significantly. In order to match the coordination number of a given rock sample, which typically is between 3 and 8 (Jerauld and Salter, 1990), it is possible to remove throats at random from a regular lattice (Dixit *et al.*, 1997,

*Author for correspondence: e-mail: m.blunt@imperial.ac.uk

1999), hence reducing the connectivity. By adjusting the size distributions to match capillary pressure data, good predictions of absolute and relative permeabilities have been reported for unsaturated soils (Fischer and Celia, 1999; Vogel, 2000).

All these models are, however, still based on a regular topology that does not reflect the random nature of real porous rock. The use of networks derived from a real porous medium was pioneered by Bryant *et al.* They extracted their networks from a random close packing of equally-sized spheres where all sphere coordinates had been measured (Bryant and Blunt, 1992; Bryant *et al.*, 1993a, b). Predictions of relative permeability, electrical conductivity and capillary pressure were compared successfully with experimental results from sand packs, bead packs and a simple sandstone. Øren and coworkers at Statoil have extended this approach to a wider range of sedimentary rocks (Bakke and Øren, 1997; Øren *et al.*, 1998). It is usually necessary to create first a three-dimensional voxel based representation of the pore space that should capture the statistics of the real rock. This can be generated directly using X-ray microtomography (Dunsmuir *et al.*, 1991; Spanne *et al.*, 1994), where the rock is imaged at resolutions of around a few microns, or by using a numerical reconstruction technique (Adler and Thovert, 1998; Øren and Bakke, 2002). From this voxel representation an equivalent network (in terms of volume, throat radii, clay content etc) can then be extracted (Delerue and Perrier, 2002; Øren and Bakke, 2002). Using these realistic networks experimental data have been successfully predicted for Bentheimer (Øren *et al.*, 1998) and Berea sandstones (Blunt *et al.*, 2002).

2. Network Model

We use a capillary dominated network model that broadly follows the work of Øren, Patzek and coworkers (Øren *et al.*, 1998; Patzek, 2001). The extensions to three-phase flow are described by Piri and Blunt (2002). Incorporation of non-Newtonian flow is discussed in Lopez *et al.* (2003). Further details, including relevant equations, can be found in Blunt (1998), Øren *et al.* (1998) and Patzek (2001). The model simulates primary drainage, wettability alteration and any subsequent cycle of water flooding, secondary drainage and gas injection.

2.1. DESCRIPTION OF THE PORE SPACE

A three-dimensional voxel representation of either Berea sandstone or a sand pack (Table I) is the basis for the networks used in this paper. The pore space image is generated by simulating the random close packing of spheres of different size followed (in the case of Berea) by compaction,

Table I. Properties of the two networks used in this paper

Network	ϕ	K(D)	Pore radius range (10^{-6} m)	Throat radius range (10^{-6} m)	Average coordination number
Sand pack	0.34	101.8	3.2–105.9	0.5–86.6	5.46
Berea	0.18	3.148	3.6–73.5	0.9–56.9	4.19

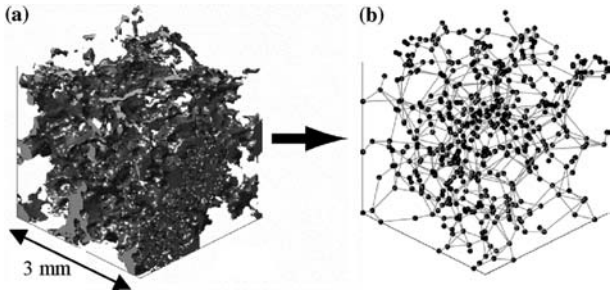

Figure 1. (a) A three-dimensional image of a sandstone with (b) a topologically equivalent network representation (Bakke and Øren, 1997; Øren *et al.*, 1998)

diagenesis and clay deposition. A topologically equivalent network of pores and throats is then generated with properties (radius, volume etc.) extracted from the original voxel representation, shown schematically in Figure 1. The networks were provided by other authors (Bakke and Øren, 1997; Øren *et al.*, 1998) – in this work we simply used them as input to our modeling studies. The Berea network represented a sample 3 mm cubed with 12,000 pores and 26,000 throats while the sand pack network contained 3,500 pores and 10,000 throats. With this relatively small number of elements, a displacement sequence can be run using standard computing resources in under a minute.

The cross-sectional shape of the network elements (pores or throats) is a circle, square or triangle with the same shape factor, $\Gamma = A/L^2$, as the voxel representation, where A is the cross sectional area and L the perimeter length. As the pore space becomes more irregular the shape factor decreases. Compared to the voxel image, the network elements are obviously only idealized representations. However, by maintaining the measured shape factor a quantitative measure of the irregular pore space is maintained. Fairly smooth pores with high shape factors will be represented by network elements with circular cross-sections, whereas more irregular pore shapes will be represented by triangular cross-sections, possibly with very sharp corners.

Using square or triangular shaped network elements allows for the explicit modeling of wetting layers where non-wetting phase occupies the center of the element and wetting phase remains in the corners. The pore space in real rock is highly irregular with wetting fluid remaining in grooves and crevices after drainage due to capillary forces. The wetting layers may only be a few microns in thickness, with little effect on the overall saturation or flow, but their contribution to wetting phase connectivity is of vital importance, ensuring low residual wetting phase saturation by preventing trapping (see, for instance, Blunt, 1998; Øren *et al.*, 1998; Patzek, 2001). Micro-porosity and water saturated clays will typically not be drained during core analysis. Rather than explicitly including this in the network representation, a constant clay volume is associated with each element. The pore and throat shapes are derived directly from the pore space representation. In this work they are not adjusted to match data. The clay volume can be adjusted to match the measured connate or irreducible water saturation after primary drainage.

3. Single-Phase Non-Newtonian Flow

There are many circumstances where non-Newtonian fluids, particularly polymers, are injected into porous media, such as for water control in oil wells or to enhance oil recovery. In this section we will predict the single-phase properties of shear-thinning fluids in a porous medium from the bulk rheology. Several authors (see, for instance, Sorbie, 1991) have derived expressions to define an apparent shear rate experienced by the fluid in the porous medium from the Darcy velocity. In practice, apparent viscosity (μ_{app}) and Darcy velocity (q) are often the measured quantities. Experimental results suggest that the overall shape of the $\mu_{app}(q)$ curve is similar to that in the bulk $\mu(\gamma)$, where γ is the shear rate. Using dimensional analysis there is a length that relates velocity to shear rate. Physically this length is related to the pore size. One estimate of this length is the square root of the absolute permeability times the porosity, $K\phi$ (Sorbie, 1991). This allows the determination of *in situ* rheograms from the bulk measured $\mu(\gamma) : \mu_{app}(q) = \mu(\gamma = q/\sqrt{K\phi})$. Many authors have remarked that this method leads to *in situ* rheograms that are shifted from the bulk curve by a constant factor, α (Sorbie, 1991; Pearson and Tardy, 2002):

$$\mu_{app}(q) = \mu\left(\gamma = \alpha q/\sqrt{K\phi}\right) \tag{1}$$

Reported values for α vary depending on the approach chosen, but experimental results suggest it generally lies in the range 1 to 15. Pearson and Tardy (2002) reviewed the different mathematical approaches used to describe non-Newtonian flow in porous media. They concluded that none

of the present continuum models give accurate estimates of bulk rheology and the pore structure and currently there is no theory that can predict its value reliably.

We will consider polymer solutions – representing Xanthan – whose bulk rheology is well-described using a truncated power-law:

$$\mu_{eff} = Max\left[\mu_{\infty}, Min\left(C\gamma^{n-1}, \mu_0\right)\right] \tag{2}$$

where C is a constant and n is a power-law exponent. We can solve analytically for the relationship between pressure drop and flow rate for a truncated power-law fluid in a circular cylinder (Lopez *et al.*, 2003). Our network models are, however, mainly composed of irregular triangular-shaped pores and throats. To account for non-circular pore shapes we replace the inscribed radius of the cylinder R in the relationship between flow rate and pressure drop with an appropriately defined equivalent radius, R_{equ}. We use an empirical approach to define R_{equ} based on the conductance, G, of the pore or throat that is exact for a circular cylinder:

$$R_{equ} = \left(\frac{8G}{\pi}\right)^{1/4} \tag{3}$$

In a network of pores and throats we do not know each pressure drop ΔP *a priori*. Hence to compute the flow and effective viscosities requires an iterative approach, developed by Sorbie *et al.* in their network model studies of non-Newtonian flow (Sorbie *et al.*, 1989). An initial guess is made for the effective viscosity in each network element. The choice of this initial value is rather arbitrary but does influence the rate of convergence, although not the final results. As a general rule, when one is interested in solving for only one flow rate across the network, the initial viscosity guess can be taken as the limiting boundary condition, μ_0 (i.e. the viscosity at very low shear rates). However, when trying to explore results for a range of increasing flow rates, the convergence process can be significantly speeded up by retaining the last solved solution for viscosity.

Once each pore and throat has been assigned an effective viscosity and conductance, the relationship between pressure drop and flow rate across each element can be found.

$$Q_i = \frac{G_i}{\mu_{eff}^i}\Delta P_i \tag{4}$$

By invoking conservation of volume in each pore with appropriate inlet and outlet boundary conditions (constant pressure), the pressure field is solved across the entire network using standard techniques. As a result the pressure drop in each network element is now known, assuming the initial guess for viscosity. Then the effective viscosity of each pore and throat is

updated and the pressure recomputed. The method is repeated until satisfactory convergence is achieved. In our case, convergence must be achieved simultaneously in all the network elements. The pressure is recomputed if the flow rate in any pore or throat changes by more than 1% between iterations. The total flow rate across the network Q_t is then computed and an apparent viscosity is defined as follows:

$$\mu_{app} = \mu_N \frac{Q_N}{Q_t} \tag{5}$$

where Q_N is the total flow rate for a simulation with the same pressure drop with a fixed Newtonian viscosity μ_N. The Darcy velocity is obtained from $q = Q_t/A$, where A is the cross sectional area of the network.

3.1. NON-NEWTONIAN RESULTS

We predict the porous medium rheology of four different experiments in the literature where the bulk shear-thinning properties of the polymers used were also provided. Two of the experiments (Hejri *et al.*, 1988; Vogel and Pusch, 1981) were performed on sand packs and for these we used the sand pack network and two were performed on Berea sandstone (Cannella *et al.*, 1988; Fletcher *et al.*, 1991), for which the Berea network was used. Table II lists the properties used to match the measured bulk rheology to a truncated power-law.

We can account for the permeability difference between our model and the systems we wish to study by realizing that simply re-scaling the network size will result in a porous medium of identical topological structure, but different permeability. To predict the experiments we generated new networks with all lengths scaled by a factor $\sqrt{K^{\exp}/K^{net}}$, where the superscripts *exp* and *net* stand for experimental and network, respectively. By construction the re-scaled network now has the same permeability as the experimental system, but otherwise has the same structure as before. Note that this is not an *ad-hoc* procedure since the scaling factor is based on the experimentally measured permeability.

Table II. Truncated power law parameters used to fit the experimental data

Experiment	C	n	μ_0 (Pa.s)	μ_∞ (Pa.s)	ϕ	K (D)
Hejri *et al.* (1988)	0.181	0.418	0.5	0.0015	0.34	0.525
Vogel and Pusch (1981)	0.04	0.57	0.1	0.0015	0.5	5
Fletcher *et al.* (1991)	0.011	0.73	0.012	0.0015	0.2	0.261
Cannella *et al.* (1988)	0.195	0.48	0.102	0.0015	0.2	0.264

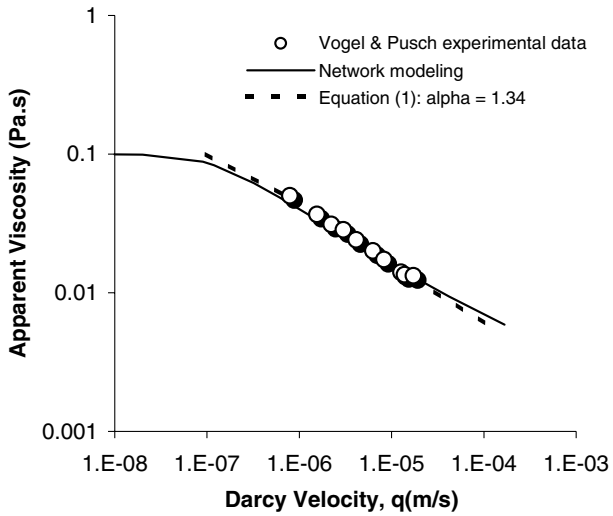

Figure 2. Comparison between network simulations (line) and the Vogel and Pusch (1981) experiments on a sand pack (circles). The dashed line is an empirical fit to the data, Equation (1), using an adjustable scaling factor α.

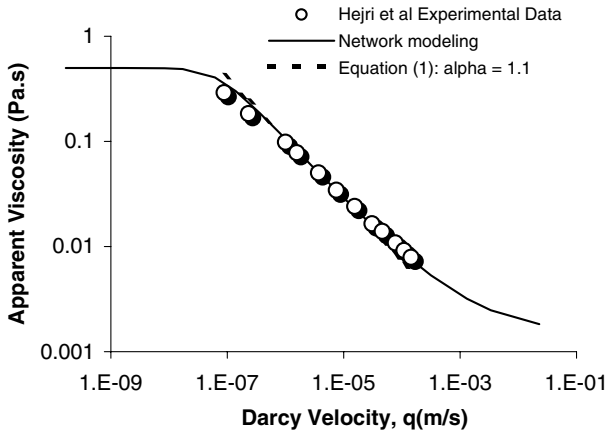

Figure 3. Comparison between network simulations (line) and the Hejri *et al.* (1988) experiments on a sand pack (circles). The dashed line is an empirical fit to the data, Equation (1), using an adjustable scaling factor α.

Figures 2–5 compare the predicted and measured porous medium rheology. Also shown are best fits to the data using Equation (1). Note that the empirical approach requires a medium-dependent parameter α to be defined, and does not accurately reproduce the whole shape of the curve. In one of the sandstone experiments – Figure 4 – the viscosity at low flow rates exceeds that measured in the bulk. This could be due to pore blocking

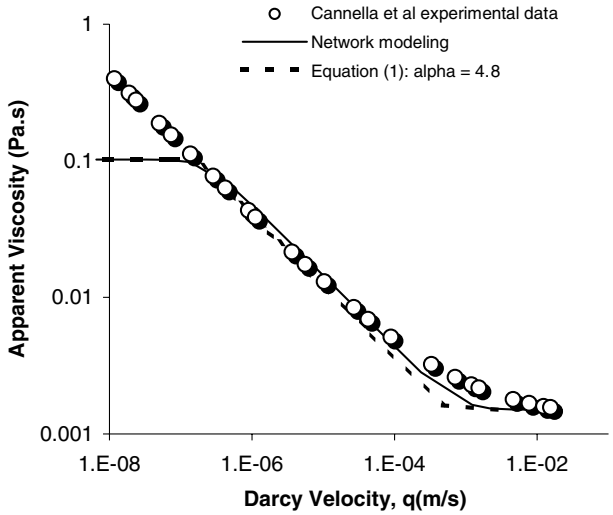

Figure 4. Comparison between network simulations (lines) and Cannella *et al.* (1988) experiments on Berea sandstone (circles). The dashed line is an empirical fit to the data, Equation (1), using an adjustable scaling factor.

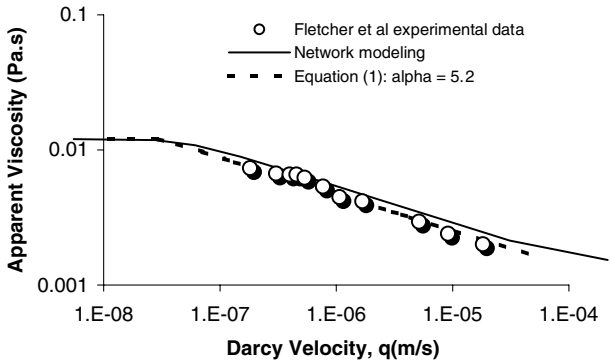

Figure 5. Comparison between network simulations (line) and the experiments of Fletcher *et al.* (1991) on Berea sandstone (circles). The dashed line is an empirical fit to the data, Equation (1), using an adjustable scaling factor α.

by polymer adsorption that we do not model. We also slightly over-predict the viscosity in the other Berea sample – Figure 5. Overall the predictions – made with no adjustable parameters – are satisfactory and indicate that the network model is capturing both the geometry of the porous medium and the single-phase non-Newtonian rheology. In the next section we will extend this approach to the more challenging case of two-phase flow, albeit with Newtonian fluids.

4. Two-Phase Flow

Two and three-phase relative permeabilities for water-wet Berea sandstone have been measured by Oak (1990). In previous work we have shown that we can predict oil/water drainage and water flood relative permeabilities accurately (Blunt *et al*., 2002; Valvatne and Blunt, 2004). In this case we know we have an appropriate network with a well-characterized wettability. The only issue is that during water injection a distribution of advancing oil/water contact angles has to be assumed – we find the uniform distribution of contact angles that matches the observed residual non-wetting phase saturation and from that predict both oil and water relative permeabilities. In this section we will show how to adjust the pore and throat size distributions to match two-phase data capillary pressure data and then predict relative permeability when we do not have an exact network representation of the medium of interest. In the following section we will predict three-phase data from Oak (1990).

When using pore-scale modeling to predict experimental data it is clearly important that the underlying network is representative of the rock. However, if the exact rock type has to be used for the network construction, the application of predictive pore-scale modeling will be severely limited due to the complexity and cost of methods such as X-ray microtomography. In this section we will use the topological information of the Berea network (relative pore locations and connection numbers) to predict the flow properties of a sand pack measured by Dury (1997) and Dury *et al.* (1998). We do not use our sand pack network, since in this case the network and the sand used in the experiments have very different properties. Capillary pressure data is used to tune the properties of the individual network elements.

Dury *et al.* (1998) measured secondary drainage and tertiary imbibition capillary pressure (main flooding cycles) and the corresponding non-wetting phase (air) relative permeabilities for an air/water system. The capillary pressures are shown in Figure 6 (Dury *et al.*, 1998). To predict the data, first all the lengths in the Berea network are scaled using the same permeability factor that was used for non-Newtonian flow. From Figure 6 it is, however, clear that the predicted capillary pressure is not close to the experimental data. This indicates the difficulty of predicting multiphase measurements – the capillary pressure and relative permeabilities are influenced by the distribution of pore and throat sizes as well as the absolute permeability. The distribution of throat sizes is subsequently modified iteratively until an adequate pressure match is obtained against the experimental drainage data (Figure 7), with individual network elements assigned inscribed radii from the target distribution while still preserving their rank order – that is the largest throat in the network is given the largest radius from the target distribution and so on. This should ensure that

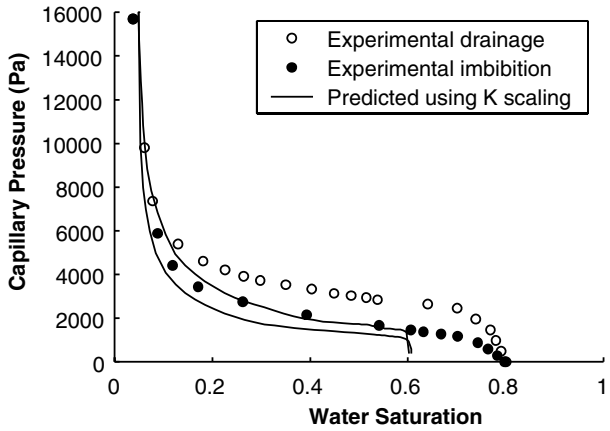

Figure 6. Comparison between predicted capillary pressures and experimental data by Dury *et al.* (1998). The size of the elements in the Berea network is modified using a scaling factor based on absolute permeability and the predictions are poor, indicating that the pore size distribution needs to be adjusted to match the data.

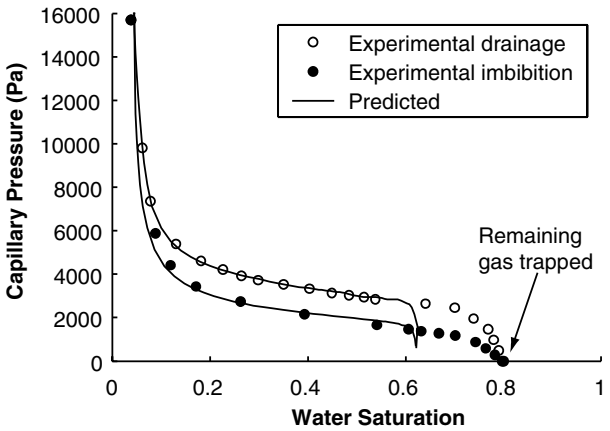

Figure 7. Comparison between predicted and measured (Dury *et al.*, 1998) capillary pressures following a network modification process to match the drainage data. Now the match is excellent, except at high water saturations. The trapped gas (air) saturation is 1 minus the water saturation when the capillary pressure is zero.

size correlations between individual elements and on larger scales are maintained. Modifications to the throat size distribution at each iteration step were done by hand rather than by any optimization technique. The results are insensitive to the details of how the throat sizes are adjusted – the final throat size distribution obtained was effectively a unique match since the rank order of size and connectivity was preserved.

Capillary pressure hysteresis is a function of both the contrast between pore body and throat radii and the contact angle hysteresis. We distribute advancing contact angles uniformly between 16 and 36 degrees, consistent with measured values by Dury (Dury, 1997; Dury *et al.*, 1998), while keeping receding values close to zero. The radii of the pore bodies is determined from Valvatne and Blunt (2004)

$$r_p = \max \left(\begin{array}{c} \beta \dfrac{\sum_{i=1}^{n_c} r_i}{n_c}, \max(r_i) \end{array} \right), \tag{6}$$

where n_c is the connection number and β is the aspect ratio between the pore body radius r_p and connecting throat radii r_i. A good match to experimental imbibition capillary pressure is achieved by distributing the aspect ratios between 1.0 and 5.0 with a mean of 2.0. This distribution is very similar to that of the original Berea network, though with a lower maximum value, which in the original network was close to 50. This is expected as the Berea network has a much larger variation in pore sizes. The absolute size of the model, defining individual pore and throat lengths, is adjusted such that the average ratio of throat length to radius is maintained from the original network. Pore and throat volumes are adjusted such that the target porosity is achieved, again maintaining the rank order.

In Figure 8 the predicted air relative permeability for secondary drainage and tertiary imbibition are compared to experimental data by Dury *et al.* (1998). The experimental data were obtained by the stationary liquid method where the water does not flow, while air is pumped through the system and the pressure drop is measured. The relative permeability hysteresis is well predicted. In imbibition snap-off disconnects the non-wetting phase leading to a lower relative permeability than in drainage. However, there are two features that we fail to match. First, the experimental trapped air saturation is much lower than predicted by the network model (Figure 7) and is lower than the value implied by the extinction point in Figure 8. Second, the extinction and emergence (when air first starts to flow) saturations are different in the experiment, while the network model predicts similar values (Figure 8). This behavior is difficult to explain physically, as the network model predicts that the trapped air saturation and the emergence and extinction points are all consistent with each other. Dury (1997) suggested that air compressibility could allow trapped air ganglia to shrink as water is injected, leading to a small apparent trapped saturation. Furthermore, air could have escaped from the end of the pack, even if the air did not span the system, leading to displacement even when the apparent air relative permeability was zero. For lower water saturations where there is more experimental confidence in the

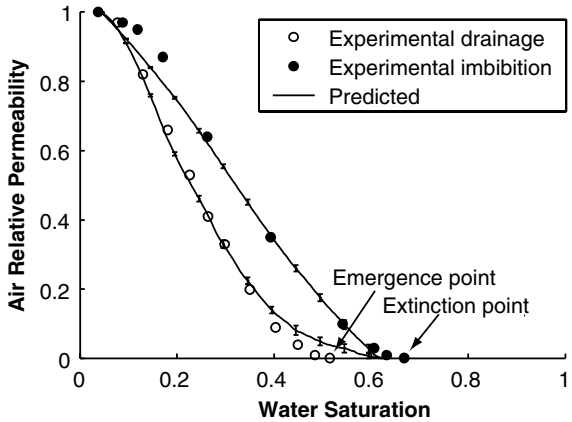

Figure 8. Comparison of network model air relative permeability predictions to experimental data measured on a sand pack by Dury *et al.* (1998). The flooding cycles shown are secondary drainage and tertiary imbibition (main cycles) and the experimental data are obtained using the stationary liquid method. The emergence point represents when gas first starts to flow during gas invasion (drainage) and the extinction point is where gas ceases to flow during imbibition.

data, the predictions are excellent and give confidence to the ability of pore-scale modeling to use readily available data (in this case capillary pressure) to predict more difficult to measure properties, such as relative permeability.

5. Three-Phase Flow

Three-phase – oil, water and gas – flow can be simulated in the network model (Piri and Blunt, 2002). All the different possible configurations of oil, water and gas in a single corner of a pore or throat are evaluated – Figures 9 and 10. Displacement is a sequence of configuration changes. For each change a threshold capillary pressure is computed (Piri and Blunt, 2002). The next configuration change is the one that occurs at the lowest invasion pressure of the injected phase. By changing what phase is injected into the network any type of displacement can be simulated (Piri and Blunt, 2002).

In this section we will predict steady-date three-phase relative permeability measured on Berea cores by Oak (1990). The two-phase oil/water data has already been predicted (Blunt *et al.*, 2002; Valvatne and Blunt, 2004) – we did not adjust any of the geometrical properties of the network (pore and throat sizes or shapes) and assumed that the receding oil/water contact angle was zero. As mentioned before, the distribution of advancing contact angles was adjusted to match the measured residual oil saturation.

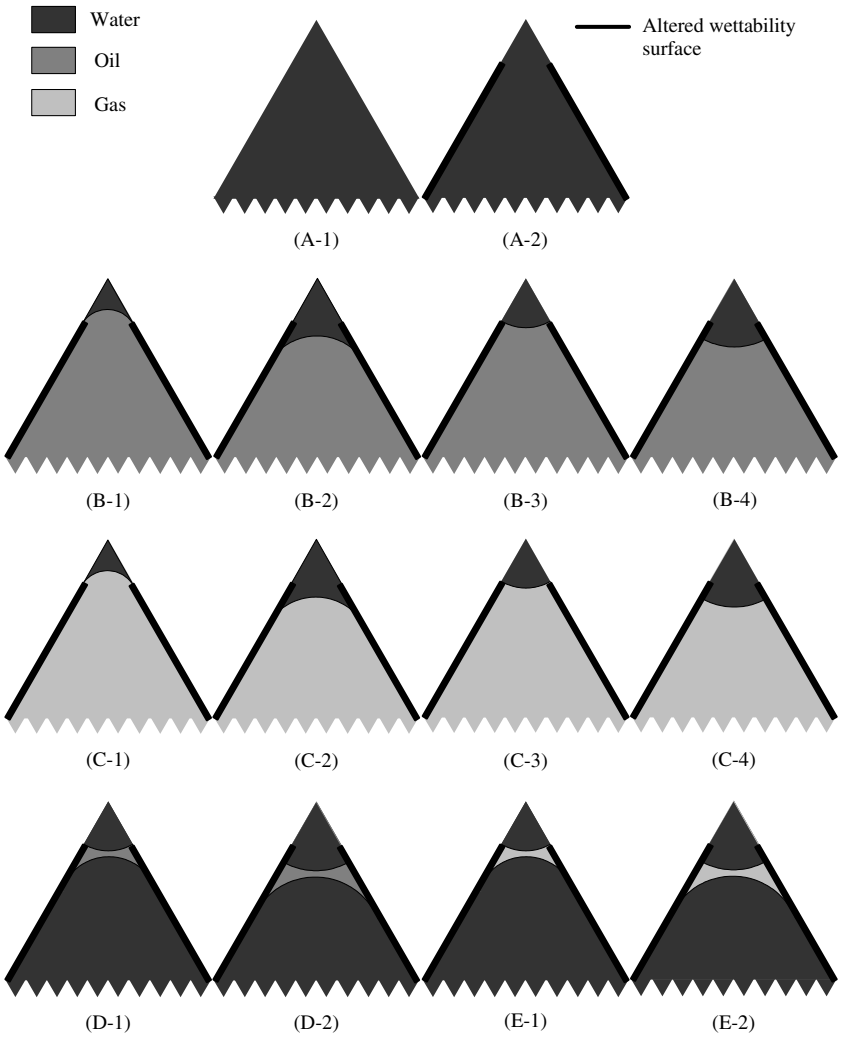

Figure 9. One- and two-phase configurations for a single corner. The bold solid line indicates regions of the surface with altered wettability. A phase may be present in the center of the pore space or as a spreading or wetting layer, sandwiched between other phases. Water is always present in the corner. The network model simulates a sequence of displacement events that represent the change from one configuration to another.

Piri and Blunt (2002) and Lerdahl *et al.* (2000) have presented three-phase predictions for this dataset – in this work we will consider a typical yet difficult case – gas injection after waterflooding – and compare predictions and experiment on a point-by-point basis. We assume that we have a spreading oil (Piri and Blunt, 2002) with oil/water and gas/oil interfacial tensions typical of light alkane/water/air systems as studied by Oak (1990). Figure 11 shows

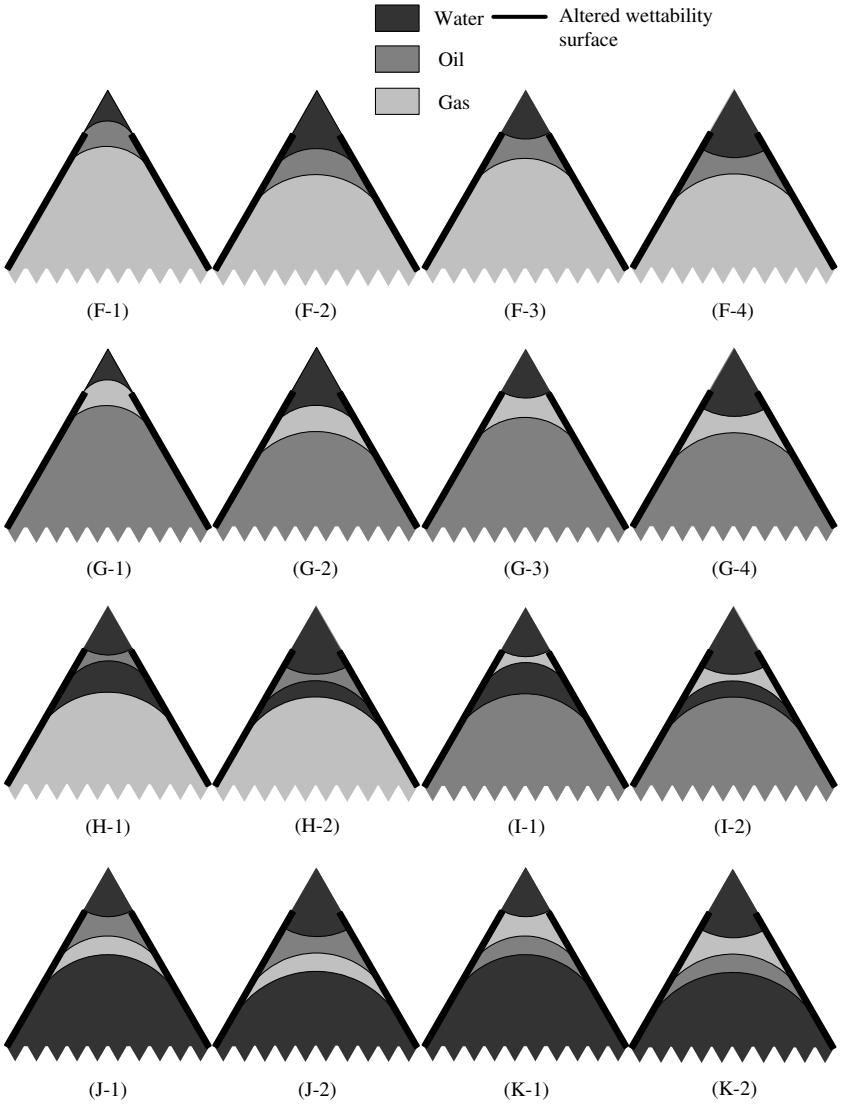

Figure 10. Three-phase configurations continued from Figure 9.

the saturation path for an experiment where gas is injected into waterflood residual oil. This is a particular challenge for pore-scale modeling since at the beginning of the displacement some of the oil is trapped and must become reconnected at the pore scale through double drainage and oil layer formation before it can be displaced (Lerdahl *et al.*, 2000; Piri and Blunt, 2002; van Dijke *et al.*, 2004). The network model simulates gas displacing either water or oil in order to track the saturation path seen experimentally.

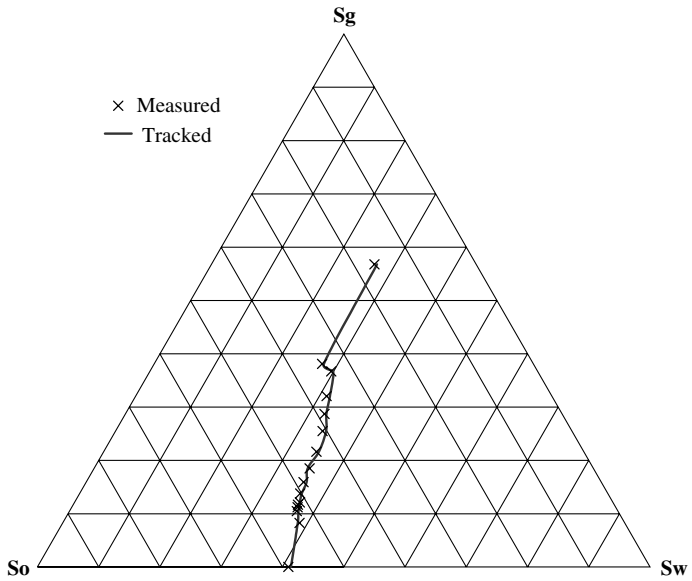

Figure 11. Saturation path for a steady-state experiment by Oak (1990) for gas injection into oil and water (crosses). The network model undergoes a series of displacements of water or oil by gas to reproduce a similar path (line).

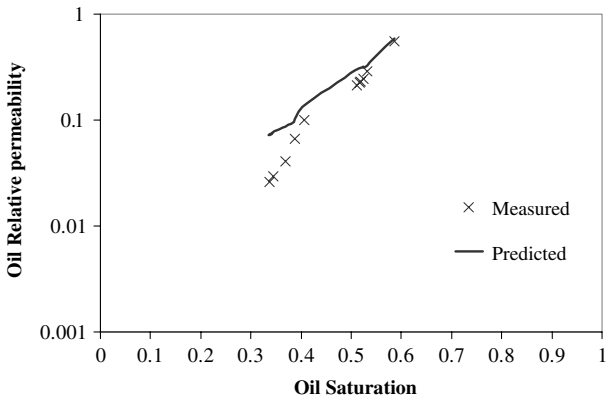

Figure 12. Experimentally measured oil relative permeability for gas injection after waterflooding (crosses) from Oak (1990) compared to predictions from network modeling (line).

Figures 12–14 show the predicted and measured three-phase oil, gas and water relative permeabilities respectively. The quality of the predictions is similar to that obtained for gas injection into higher initial oil saturations (Piri and Blunt, 2002). The three-phase predictions are satisfactory, although not as good as for two-phase flow. This is because the pore scale physics is more complex and uncertain when three phases are flowing – in

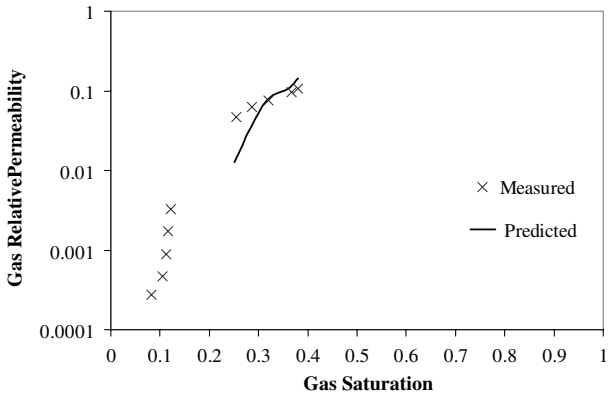

Figure 13. Experimentally measured gas relative permeability for gas injection after waterflooding (crosses) from Oak (1990) compared to network model predictions (line).

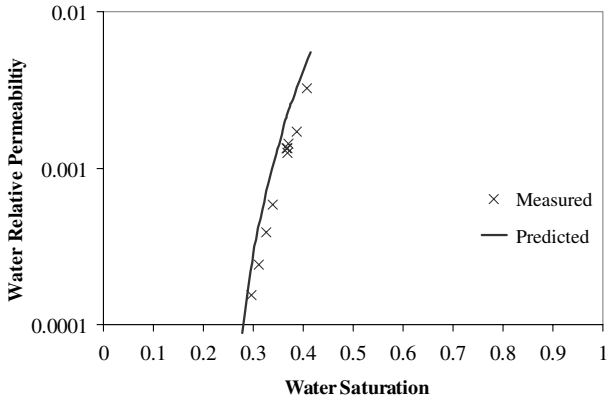

Figure 14. Experimentally measured water relative permeability for gas injection after waterflooding (crosses) from Oak (1990) compared to network model predictions (line).

particular we do not know how well the fluid configurations in Figure 10 represent the true arrangements of fluid.

For the oil relative permeability, Figure 12, the network model tends to over-predict the relative permeability at low saturation. At low oil saturation the oil is flowing in layers (see Figure 10G) and the relative permeability is controlled by our assumptions of layer connectivity and conductance. It appears that we over-estimate the connectivity of the layers and that in reality oil layers do not have the rather high effective conductance that we assume using our idealized model of the pore space geometry. The gas relative permeability is well predicted at high gas saturation. However, at low saturation finite size effects in the network mean

that we predict that gas is not connected even though it does flow in the experiments. The predictions of water relative permeability are excellent.

6. Discussion and Conclusions

We have demonstrated that pore-scale modeling combined with geologically realistic networks can reliably predict single-, two- and three-phase data for water-wet media. The predictions of the single-phase shear thinning rheology of polymer solutions in porous media were excellent and superior to empirical scaling approaches, since the results did not depend on an unknown porous-medium-dependent factor. For two-phase flow the results were also excellent if the pore structure of the porous medium is known, although the distribution of contact angles for waterflooding needs to be estimated. If the pore structure is not known *a priori*, we showed how to adjust the pore size distribution to match capillary pressure data and then use this to make good predictions of relative permeability. For three-phase flow modeling is more of a challenge because of the complexity of the pore-scale physics. However, we were able to predict relative permeabilities with reasonable accuracy for gas injection after waterflooding.

We did not address wettability in this paper. Most natural media that have been in contact with oil or other non-aqueous phase liquids change their wettability and often display mixed-wet or oil-wet characteristics. The network model presented in this paper can handle media of any wettability and has made accurate predictions of relative permeability and oil recovery for mixed-wet reservoir samples (Piri and Blunt, 2002; Valvatne and Blunt, 2004). Figures 9 and 10 show all the possible two- and three-phase configurations including wettability alteration: after primary drainage, where oil contacts the solid surface directly the oil/water contact angle may change to any value (indicated by the bold lines in Figures 9 and 10). During gas injection different gas/oil and gas/water contact angles can also be assigned to these regions (Piri and Blunt, 2002). Regions of the pore space that remain water filled remain water-wet. Extensive experimental verification of the models for media of different wettability, particularly for three-phase flow, remains the subject of future study.

The aim of pore-scale modeling is to predict properties that are difficult to measure, such as relative permeability, from more readily available data, such as drainage capillary pressure. In addition, the model can readily be used to predict the changes in flow properties as the pore structure or wettability varies. As such it can be used to characterize multiphase properties in geological models. We have already shown that using pore-scale modeling to characterize variations in relative permeability leads to significantly different predictions of recovery at the field scale than traditional empirical modeling approaches (Blunt *et al.*, 2002).

Acknowledgements

The members of the Imperial College Consortium on Pore-Scale Modelling (BHP, Gaz de France, JNOC, PDVSA-Intevep, Schlumberger, Shell, Statoil, the UK Department of Trade and Industry and the EPSRC) are thanked for their financial support. We also thank Pål-Eric Øren (Statoil) for sharing his network data with us.

References

Adler, P. M. and Thovert, J. F.: 1998, Real porous media: Local geometry and macroscopic properties, *Appl. Mechanics Rev.* **51**(9), 537–585.

Bakke, S. and Øren, P. E.: 1997, 3-D pore-scale modelling of sandstones and flow simulations in the pore networks, *SPE Journal* **2**(2), 136–149.

Blunt, M. J.: 1998, Physically-based network modeling of multiphase flow in intermediate-wet porous media, *J. Petrol. Sci. Eng.* **20**(3–4), 117–125.

Blunt, M. J., Jackson, M. D., Piri, M. and Valvatne, P. H.: 2002, Detailed physics, predictive capabilities and macroscopic consequences for pore-network models of multiphase flow, *Adv. Water Resour.* **25**(8–12), 1069–1089.

Bryant, S. and Blunt, M.: 1992, Prediction of relative permeability in simple porous-media, *Phys. Rev. A* **46**(4), 2004–2011.

Bryant, S. L., King, P. R., and Mellor, D. W.: 1993a, Network model evaluation of permeability and spatial correlation in a real random sphere packing, *Transport in Porous Media* **11**(1), 53–70.

Bryant, S. L., Mellor, D. W., and Cade, C. A.: 1993b Physically representative network models of transport in porous-media, *AIChE Journal* **39**(3), 387–396.

Cannella, W. J., Huh, C. and Seright, S.: 1988, Prediction of xanthan rheology in porous media, Paper SPE 18089, in: *Proceedings of the 63rd Annual Technical Conference and Exhibition of the Society of Petroleum Engineers*, Houston, TX, USA.

Chatzis, I. and Dullien, F. A. L.: 1997, Modelling pore structures by 2-D and 3-D networks with application to sandstones, *J. Can. Petrol. Technol.* **16**(1), 97–108.

Delerue, J. F. and Perrier, E.: 2002, DXSoil, a library for 3D image analysis in soil science, *Comp. Geosci.* **28**(9), 1041–1050.

Dixit, A. B., McDougall, S. R., and Sorbie, K. S.: 1997, Pore-level investigation of relative permeability hysteresis in water-wet systems, SPE 37233, in: *Proceedings of the 1997 SPE International Symposium on Oilfield Chemistry*, February 1997, Houston.

Dixit, A. B. et al.: Pore-scale modeling of wettability effects and their influence on oil recovery, *SPE Reserv. Eval. Eng.* **2**(1), 25–36.

Dunsmuir, J. H. et al.: 1991, X-ray microtomography. A new tool for the characterization of porous media, SPE 22860, in: *Proceedings of the 1991 SPE Annual Technical Conference and Exhibition*, October 1991, Dallas.

Dury, O.: 1997, Organic pollutants in unsaturated soils: Effect of butanol as model contaminant on phase saturation and flow characteristics of a quartz sand packing, PhD Thesis, ETH Zürich.

Dury, O., Fischer, U. and Schulin, R.: 1998, Dependence of hydraulic and pneumatic characteristics of soils on a dissolved organic compound, *J. Contam. Hydrol* **33**(1–2), 39–57

Fischer, U. and Celia, M. A.: 1999, Prediction of relative and absolute permeabilities for gas and water from soil water retention curves using a pore-scale network model, *Water Resour. Res.* **35**(4), 1089–1100.

Fletcher, A. J. P. et al.: 1991, Measurements of polysaccharide polymer properties in porous media, Paper SPE 21018, in: *Proceedings of the Society of Petrol. Engineers International Symposium on Oilfield Chemistry*, Anaheim, California, USA.

Hejri, S., Willhite, G. P. and Green, D. W.: 1988, Development of correlations to predict biopolymer mobility in porous media, Paper SPE 17396, in: *Proceedings of the Society of Petroleum Engineers Enhanced Oil Recovery Symposium* , Tulsa, USA.

Jerauld, G. R. and Salter, S. J.: 1990, Effect of pore-structure on hysteresis in relative permeability and capillary pressure. Pore-level modeling, *Transport in Porous Media* **5**(2), 103–151.

Lerdahl, T. R., Øren, P. E., and Bakke, S.: 2000, A predictive network model for three-phase flow in porous media, SPE 59311, in: *Proceedings of the SPE/DOE Symposium on Improved Oil Recovery*, April 2–5, Tulsa.

Lopez, X. P., Valvatne, P. H. and Blunt, M. J.: 2003, Predictive network modeling of single-phase non-Newtonian flow in porous media, *J. Colloid and Interf. Sci.* **264**(1), 256–265.

Oak, M. J.: 1990, Three-phase relative permeability of water-wet Berea, SPE 20183, in: *Proceedings of the SPE/DOE Seventh Symposium on Enhanced Oil Recovery*, 28 April, Tulsa.

Øren, P. E. and Bakke, S.: 2002, Process based reconstruction of sandstones and prediction of transport properties, *Transport in Porous Media* **46**(2–3), 311–343.

Øren, P. E., Bakke, S. and Arntzen, O. J.: 1998, Extending predictive capabilities to network models, *SPE Journal* **3**(4), 324–336.

Patzek, T. W.: 2001, Verification of a complete pore network simulator of drainage and imbibition, *SPE Journal* **6**(2), 144–156.

Pearson, J. R. A. and Tardy, P. M. J.: 2002, Models for flow of non-Newtonian and complex fluids through porous media, *J. Non-Newton. Fluid Mechanics* **102**: 447–473.

Piri, M. and Blunt, M. J.: 2002, Pore-scale modeling of three-phase flow in mixed-wet systems, Paper SPE 77726, in: *Proceedings of the SPE Annual Meeting*, 29 September–2 October San Antonio, Texas.

Sorbie, K. S.: 1991, *Polymer-Improved Oil Recovery,* CRC Press Inc.

Sorbie, K. S., Clifford, P. J. and Jones, E. R. W.: 1989, The rheology of pseudoplastic fluids in porous media using network modeling, *J. Colloid Interf. Sci.* **130**(2): 508–534.

Spanne, P. et al.: 1994, Synchrotron computed microtomography of porous-media – topology and transports, *Phy. Rev. Lett.* **73**(14), 2001–2004.

Valvatne, P. H. and Blunt, M. J.: 2004, Predictive pore-scale network modeling of two-phase flow in mixed wet media, *Water Resources Res.* **40**, W07406, DOI: 10.1029/2003 WR002627.

van Dijke, M. I. J., Sorbie, K. S., Sohrabi, M. and Danesh, A.: 2004, Three-phase flow in WAG processes in mixed-wet porous media: pore scale network simulations and comparison with water-wet micromodel experiments, SPE 75192, in: *Proceedings of the SPE/DOE Conference on Improved Oil Recovery*, April, Tulsa, OK.

Vogel, H. J.: 2000, A numerical experiment on pore size, pore connectivity, water retention, permeability, and solute transport using network models, *Eur. J. Soil Sci.* **51**(1), 99–105.

Vogel, P. and Pusch, G.: 1981, Some aspects of non-Newtonian fluids in porous media, in: *Proceedings of the First European Symposium on EOR*, September 1981, Bournemouth, UK.

Wilkinson, D. and Willemsen, J. F.: 1983, Invasion percolation – a new form of percolation theory, *J. Phy. A: Math. Gen.* **16**(14), 3365–3376.